Cell transformation by FLT3 ITD in acute myeloid leukemia involves oxidative inactivation of the tumor suppressor protein-tyrosine phosphatase DEP-1/ PTPRJ

Rinesh Godfrey,[1] Deepika Arora,[1] Reinhard Bauer,[1,2] Sabine Stopp,[1] Jörg P. Müller,[1] Theresa Heinrich,[1] Sylvia-Annette Böhmer,[1] Markus Dagnell,[3] Ulf Schnetzke,[4] Sebastian Scholl,[4] Arne Östman,[3] and Frank-D. Böhmer[1]

[1]Institute of Molecular Cell Biology, Center for Molecular Biomedicine, Jena University Hospital, Jena, Germany; [2]Center for Sepsis Control and Care, Jena University Hospital, Jena, Germany; [3]Cancer Center Karolinska, Karolinska Institutet, Stockholm, Sweden; and [4]Department of Hematology/Oncology, Clinic for Internal Medicine II, Jena University Hospital, Jena, Germany

Signal transduction of *FMS*-like tyrosine kinase 3 (FLT3) is regulated by protein-tyrosine phosphatases (PTPs). We recently identified the PTP DEP-1/CD148/ PTPRJ as a novel negative regulator of FLT3. This study addressed the role of DEP-1 for regulation of the acute myeloid leukemia (AML)–related mutant FLT3 internal tandem duplication (ITD) protein. Our experiments revealed that DEP-1 was expressed but dysfunctional in cells transformed by FLT3 ITD. This was caused by enzymatic inactivation of DEP-1 through oxidation of the DEP-1 catalytic cysteine. In intact cells, including primary AML cells, FLT3 ITD kinase inhibition reactivated DEP-1. DEP-1 reactivation was also achieved by counteracting the high levels of reactive oxygen species (ROS) production detected in FLT3 ITD–expressing cell lines by inhibition of reduced NAD phosphate (NADPH)–oxidases, or by overexpression of catalase or peroxiredoxin-1 (Prx-1). Interference with ROS production in 32D cells inhibited cell transformation by FLT3 ITD in a DEP-1–dependent manner, because RNAi-mediated depletion of DEP-1 partially abrogated the inhibitory effect of ROS quenching. Reactivation of DEP-1 by stable overexpression of Prx-1 extended survival of mice in the 32D cell/C3H/HeJ mouse model of FLT3 ITD–driven myeloproliferative disease. The study thus uncovered DEP-1 oxidation as a novel event contributing to cell transformation by FLT3 ITD. (*Blood*. 2012;119(19): 4499-4511)

Introduction

Acute myeloid leukemia (AML) is the most frequent leukemia in adults with improving but still limited treatment possibilities, notably in elderly patients.[1,2] It arises by malignant transformation of myeloid progenitor cells. Among the contributing genetic lesions, mutations in the class III receptor tyrosine kinase (RTK) *FMS*-like tyrosine kinase 3 (FLT3) occur in approximately 30% of patients.[3] The prevalent type of FLT3 mutations are internal tandem duplications (ITD) of amino acid stretches in the juxtamembrane domain or in the tyrosine kinase domain,[4,5] which confer cytokine-independent proliferation and resistance to apoptosis, and causally contribute to AML in combination with additional genetic lesions.[1] Compared with the ligand-activated wild-type (WT) FLT3, FLT3 ITD mutants exhibit not only elevated but also altered signaling quality, with very pronounced activation of signal transducer and activator of transcription (STAT)5 as one characteristic feature.[6,7] FLT3 ITD also causes the production of high levels of reactive oxygen species (ROS).[8,9]

Signal transduction of RTKs is regulated by protein-tyrosine phosphatases (PTPs). PTPs prevent ligand-independent RTK activation, and contribute to modulation and termination of ligand-induced signaling.[10] The activity of PTPs is regulated at several different levels.[11] One regulatory principle is the reversible oxidation of the PTP active-site cysteine, which leads to reversible inactivation.[12,13] Temporary inactivation of negatively regulating PTPs by this mechanism is believed to be important for efficient RTK signal propagation in the cell.[14] A major ROS causing cellular PTP oxidation is hydrogen peroxide (H_2O_2), which can be generated by a dismutase reaction from superoxide anions, the reaction products of NADPH-oxidases. Activation of the NADPH oxidase isoform 1 (NOX1) occurs downstream of RTK activation, and involves activation and membrane translocation of the small guanosine triphosphate (GTP)ase Rac1.[15] ROS generation in the cell is counteracted by efficient ROS decomposing systems.[16] These include peroxiredoxins (Prx), which have a very low K_m for H_2O_2 and can eliminate it even at low concentrations.[17]

Relatively little is known about PTPs regulating FLT3 signal transduction. We have previously shown that the nontransmembrane PTPs PTP1B and SHP-1 can potently dephosphorylate FLT3 on overexpression. Further, PTP1B appears important for suppressing signaling of newly synthesized FLT3.[7,18] SHP-2 acts as a positive regulator, because it is important for Erk activation and proliferation induced by ligand-activated WT FLT3. However, it is dispensable for FLT3 ITD–mediated transformation.[19] We previously performed a shRNA-based screen to identify PTPs regulating WT FLT3. The initial screen assessed the effects of shRNAs for 20 PTPs on FL-induced Erk1/2 activation in WT FLT3-expressing 32D cells. Among several potentially relevant PTPs, we validated and characterized density-enhanced phosphatase-1 (DEP-1, systematic name PTPRJ, also CD148) as a negative regulator of WT FLT3 autophosphorylation and signaling.[20]

Submitted February 11, 2011; accepted March 11, 2012. Prepublished online as *Blood* First Edition paper, March 20, 2012; DOI 10.1182/blood-2011-02-336446.

The online version of this article contains a data supplement.

The publication costs of this article were defrayed in part by page charge payment. Therefore, and solely to indicate this fact, this article is hereby marked "advertisement" in accordance with 18 USC section 1734.

In this study the role of DEP-1 for regulation of FLT3 ITD, the AML-related mutant version of FLT3 was explored. The experiments revealed that DEP-1 was expressed but not functioning as a PTP for FLT3 ITD. The high ROS levels in FLT3 ITD–expressing cells led to partial inactivation of DEP-1 by reversible oxidation. Blocking ROS formation with different approaches restored DEP-1 activity and attenuated transformation in vitro and in vivo. Our findings reveal the reversible inactivation of a tumor-suppressive PTP as a previously unrecognized mechanism which contributes to cell transformation by FLT3 ITD.

Methods

Cell lines

HEK293, HEK293T cells, and the human AML cell lines, EOL-1, THP-1, RS4-11, MOLM-13, and MV4-11 were purchased from German Collection of Microorganisms and Cell Cultures (DSMZ). The Phoenix Ampho packaging cell line was a kind gift of Dr G. Nolan (Stanford University Medical Center, Stanford, CA). AML cell lines were maintained in RPMI-1640 (Biochrom) with 10% heat-inactivated fetal bovine serum (FBS) with the exception of RS4-11, which was maintained in Alpha MEM (GIBCO-BRL) with 10% heat inactivated FBS. HEK 293 and Phoenix Ampho were maintained in DMEM/F12 (GIBCO-BRL) with 10% FBS. 32D mouse hematopoietic progenitor cells stably expressing murine FLT3-WT or FLT3 ITD were a kind gift of Dr J. Duyster (Technical University of Munich, Munich, Germany) and were maintained in HEPES (*N*-2-hydroxyethylpiperazine-*N*′-2-ethanesulfonic acid)–buffered RPMI-1640 (Biochrom) with 10% heat-inactivated FBS, 1mM sodium pyruvate, and 2.5 ng/mL murine recombinant IL3 (Peprotech). 32D cells expressing human WT FLT3 or FLT3 ITD were previously described,[20] and were used for FLT3 autophosphorylation experiments.

AML patient samples

Leukemic cells from AML patient blood were isolated by Ficoll (Biochrom) density gradient separation by standard procedures and processed for the experiments within 2 to 3 hours after taking. The patient study was approved by the local ethics committee and each patient gave written informed consent. The characteristics of AML patients included in this study are summarized in supplemental Table 1 (available on the *Blood* Web site; see the Supplemental Materials link at the top of the online article). Determination of the FLT3 mutation status is outlined in supplemental Methods.

DNA constructs

Plasmids encoding WT hFLT3, hFLT3 ITD,[18] and HA-tagged hDEP-1[21] were previously described. The human NOX4 expression construct was a kind gift of Dr David Lambeth (Emory University Medical School, Atlanta, GA). The construct encoding a fluorescent sensor (HyPer-cyto), capable for highly specific detection of H_2O_2, was from Evrogen. A vector encoding dominant negative (dn) STAT5 was a kind gift of Dr Edith Pfitzner (Institute for Biochemistry, CMB, Jena University, Germany). Retroviral vectors encoding dnRac-1 and rat Prx-1 were kindly provided by Dr Henrik Ungefroren (Department of General and Thoracic Surgery, University Hospital Kiel, Kiel, Germany), and Dr Jack van Horssen (VU University Medical Center, Amsterdam, The Netherlands), respectively. A full-length *PTPRJ*-promoter reporter construct was previously described.[21] shRNA constructs for knockdown of endogenous DEP-1 in 32D cells were previously reported.[20]

Antibodies and reagents

Antibodies and reagents are described in supplemental Methods.

Transient transfections and generation of cell lines with altered gene expression

Transient transfections were carried out using branched polyethylenimine (PEI; Sigma-Aldrich; 40872-7) as previously described.[21] Further details are described in supplemental Methods.

ROS measurements

Measurements in HEK293 cells. The use of the HyPer vector and the detection of ROS with carboxy-H_2DFFDA and confocal microscopy are described in supplemental Methods.

Detection of ROS with carboxy-H_2DFFDA and a fluorescence plate reader. This method was used to analyze suspension cells. Cells were washed with serum-free RPMI-1640 medium, and starved for 4 hours. Inhibitor treatments were made simultaneously during this starvation time. After that, cells were washed twice with Krebs Ringer phosphate glucose buffer (KRPG; 145mM NaCl, 5.7mM KH_2PO_4, 4.86mM KCl, 0.54mM $CaCl_2$, 1.22mM $MgSO_4$, 5.5mM glucose), and then resuspended in 1 mL KRPG (2×10^6 cells/assay point). Carboxy-H_2DFFDA (20μM) was added, the suspension mixed well, and then incubated in dark for 20 to 30 minutes at room temperature. The subsequent steps were strictly carried out in dark. The cells were washed twice with KRPG and transferred to a 12-well dish. The fluorescence intensity was quantified with a fluorescence microplate reader (TECAN Infinite 200 plate reader) with excitation at 485 nm and emission at 530 nm.

PTP activity measurements

All the PTP activity-related work was carried out in an anaerobic chamber, Glovebox P10 R215T2s (TGS Glovebox Systemtechnik GmbH). Cells were lysed using deoxygenated lysis buffer in the anaerobic chamber. The lysates were then subjected to immunoprecipitation of different PTPs. The immunoprecipitates were washed and then used for PTP activity assay using the Tyrosine Phosphatase assay system (Promega Corporation). Control precipitations with nonspecific immunoglobulin (Ig)G were carried out and assayed in parallel, and the activity values were subtracted from those for specific immunoprecipitates. Alternatively, PTP activity was assayed with a ^{32}P-labeled peptide substrate as previously described.[22] General PTP oxidation was assessed using the "modified PTP in-gel assay,"[13] and PTEN oxidation was measured based on mobility alteration and with an alkylation method. A detailed description of these methods is provided in supplemental Methods.

Biotin labeling of the DEP-1 catalytic cysteine

DEP-1 was labeled with biotin using a previously described method[23] with several modifications. In brief, cells were lysed using deoxygenated lysis buffer at pH 5.5 containing 5mM EZ-Link iodoacetyl-PEG_2-biotin. After allowing complete alkylation of reactive thiols, the lysate was used for DEP-1 immunoprecipitation. Finally, biotin labeling was detected using antibiotin antibodies. A detailed description is provided in supplemental Methods.

Proliferation and colony formation assays

These are described in supplemental Methods.

Animal experiments

Animal experiments were carried out as described.[7] Eight- to 10-week-old C3H/HeJ mice (The Jackson Laboratory), which are syngenic to 32D cells, were used to assess the in vivo development of myeloproliferative disease (MPD). 32D cells (2×10^6) engineered as described in the figure legend of Figure 7 and expressing equal levels of mFLT3 ITD (sorted for equal receptor expression) were injected into the lateral tail vein. The experiments were performed in accordance with the Animal Welfare Guidelines and were approved by the local ethics committee of the regional government of

Thuringia. To assess DEP-1 knockdown levels at the end of experiment, spleen cells were fluorescence-activated cell sorter (FACS)–sorted to enrich the GFP-expressing 32D FLT3 ITD cells, expanded for 2 days in culture and subjected to immunoblotting and quantitative qRT-PCR (qRT-PCR) based detection of DEP-1 mRNA expression as described in supplemental Methods.

Results

Dysfunction of DEP-1 in FLT3 ITD–expressing cells

We recently identified DEP-1 as a negative regulator of FLT3 phosphorylation, and FLT3 signaling among 20 PTPs screened by a shRNA-based knockdown approach in 32D murine myeloid progenitor cells expressing WT FLT3.[20] Negative control of FLT3 signaling is exemplified by hyperphosphorylation of WT FLT3 in DEP-1 depleted cells (Figure 1A).[20]

To address if DEP-1 also acts as a negative regulator of FLT3 ITD we explored the effect of DEP-1 knockdown on FLT3 ITD phosphorylation. Surprisingly, no alteration of the constitutively high FLT3 ITD phosphorylation could be observed, despite the efficient knockdown of DEP-1 by shRNA expression (Figure 1B). Similarly, DEP-1 knockdown in the FLT3 ITD–expressing human MV4-11 cell line did not affect the level of FLT3 ITD autophosphorylation (Figure 1C). These findings suggested that DEP-1 knockdown may not affect FLT3 ITD mediated transformation. This was tested in FLT3 ITD–expressing 32D cells. Transformation of these cells is associated with efficient formation of colonies in methylcellulose, and by development of a MPD on injection of the cells into syngeneic C3H mice. Strongly reduced DEP-1 levels did indeed, neither affect colony formation (supplemental Figure 1B) nor MPD development in vivo (data not shown, see also Figure 7C).

These findings were compatible with the presence of inactive DEP-1 in FLT3 ITD–expressing cells. A set of experiments was therefore performed, which analyzed the impact of FLT3 ITD on the activity of DEP-1.

PTP-activity analysis of immunoprecipitated DEP-1 demonstrated significantly reduced DEP-1 activity in FLT3 ITD–expressing 32D cells compared with parental 32D cells or WT FLT3-expressing 32D cells (Figure 1D). To test a possibly more general character of this phenomenon and to enable mechanistic studies, we also performed experiments in HEK293 cells. Also in these cells, DEP-1 activity was clearly reduced in the presence of FLT3 ITD, without noticeable effects on DEP-1 protein levels (Figure 1E, supplemental Figure 2A). FLT3 ITD did not affect the activity of a reporter construct harboring the DEP-1 promoter (supplemental Figure 2B), or DEP-1 mRNA levels assayed by qRT-PCR (supplemental Figure 2C). The analysis of DEP-1 mRNA in AML patient samples by qRT-PCR revealed a large variation in expression but no significant differences related to the FLT3 ITD status (supplemental Figure 2D). In normal $CD34^+$ progenitor cells we detected comparatively low DEP-1 mRNA levels (supplemental Figure 2D), precluding assessment of DEP-1 activity from technical reasons. Our observation is consistent with earlier reports indicating highly variable DEP-1 expression in different hematopoietic cell populations, with high expression in myeloid and B cells.[24,25] Normal $CD34^+$ cells and AML cells have recently been reported to exhibit strikingly different mRNA expression profiles.[26]

Taken together, the described findings supported the notion that FLT3 ITD causes reduced DEP-1 activity compared with cells expressing WT FLT3 rather than alterations in mRNA or protein levels.

FLT3 ITD induces high levels of ROS

Given the high sensitivity of PTPs to oxidative inactivation,[14] and recently reported elevated ROS levels in FLT3 ITD–expressing cells,[8,9] it appeared possible that DEP-1 inactivation in FLT3 ITD cells was caused by elevated ROS levels. To investigate this possibility, we first characterized the effects of FLT3 ITD on ROS production in different cell models.

High levels of ROS production were detectable with the fluorescent dye 5-(and-6)-carboxy-2′,7′-difluorodihydrofluorescein diacetate (carboxy-H_2DFFDA) in 32D cells stably expressing FLT3 ITD, whereas much lower levels of ROS were detectable in the corresponding parental 32D cells, or 32D cells stably expressing FLT3 WT (Figure 2A). In addition, overexpression of FLT3 ITD (but not WT FLT3) in HEK293 cells resulted in elevated fluorescence of a hydrogen peroxide (H_2O_2) sensitive GFP, expressed from the vector pHyPer,[27] which was comparable with a signal induced by overexpression of the constitutively active NOX isoform NOX4 (supplemental Figure 3A).[15]

Importantly, the human AML cell lines MV4-11 and MOLM13 harboring FLT3 ITD also produced high levels of ROS, whereas the AML lines THP-1, RS4-11, and EOL-1, which express WT FLT3, exhibited lower ROS levels (Figure 2B). Finally, primary blasts from AML patients expressing FLT3 ITD had a clear trend to higher ROS-levels than blasts from patients with WT FLT3 (Figure 2C). Comparison with FLT3 ITD allele-load revealed some positive correlation in that the 4 patients with highest allele loads also showed highest ROS levels (supplemental Figure 4A black bars). It should be noted that these measurements were not side-by-side comparisons, which may have obscured larger differences, as they were observed in a previous study.[8]

To identify possibilities of interference with FLT3 ITD–induced ROS production, we tested inhibition of several components of FLT3 ITD–dependent signaling.

Inhibition of FLT3 ITD kinase activity with the selective class III RTK inhibitor AG1295, treatment of the cells with diphenylene iodonium (DPI), a flavoprotein inhibitor which potently blocks NOX activity,[28] or with the general antioxidant 6-hydroxy-2,5,7,8-tetramethylchroman-2-carboxylic acid (TROLOX) potently suppressed FLT3 ITD-driven ROS production (supplemental Figure 3B-C). Similar effects were obtained after transfection with a dn form of the small GTPase Rac1 (RacN17) and on treatment with the PI3-kinase inhibitor wortmannin, but not with UO126, an inhibitor of the MAPK pathway (supplemental Figure 3B-C). Overexpression of a dnSTAT5 protein, or treatment of the cells with a small-molecule STAT5 antagonist[29] also reduced ROS production in presence of FLT3 ITD (supplemental Figure 3B-C).

We also tested if activation of WT FLT3 would cause ROS production and had any effect on DEP-1 activity. Stimulation of WT FLT3–expressing 32D cells with FL indeed led to a small, but significant increase in detectable ROS, but this was not accompanied by an alteration in DEP-1 activity (supplemental Figure 3D).

FLT3 ITD–induced ROS is required for DEP-1 inactivation

The findings described above suggested that FLT3 ITD–induced ROS was involved in the FLT3 ITD–dependent inactivation of DEP-1. To directly test this idea, a set of experiments was performed analyzing if alterations in ROS production, or ROS scavenging would affect DEP-1 activity in FLT3 ITD–expressing cells.

In an initial experiment, catalase overexpression was used as an approach for ROS scavenging. Interestingly, catalase quenched the

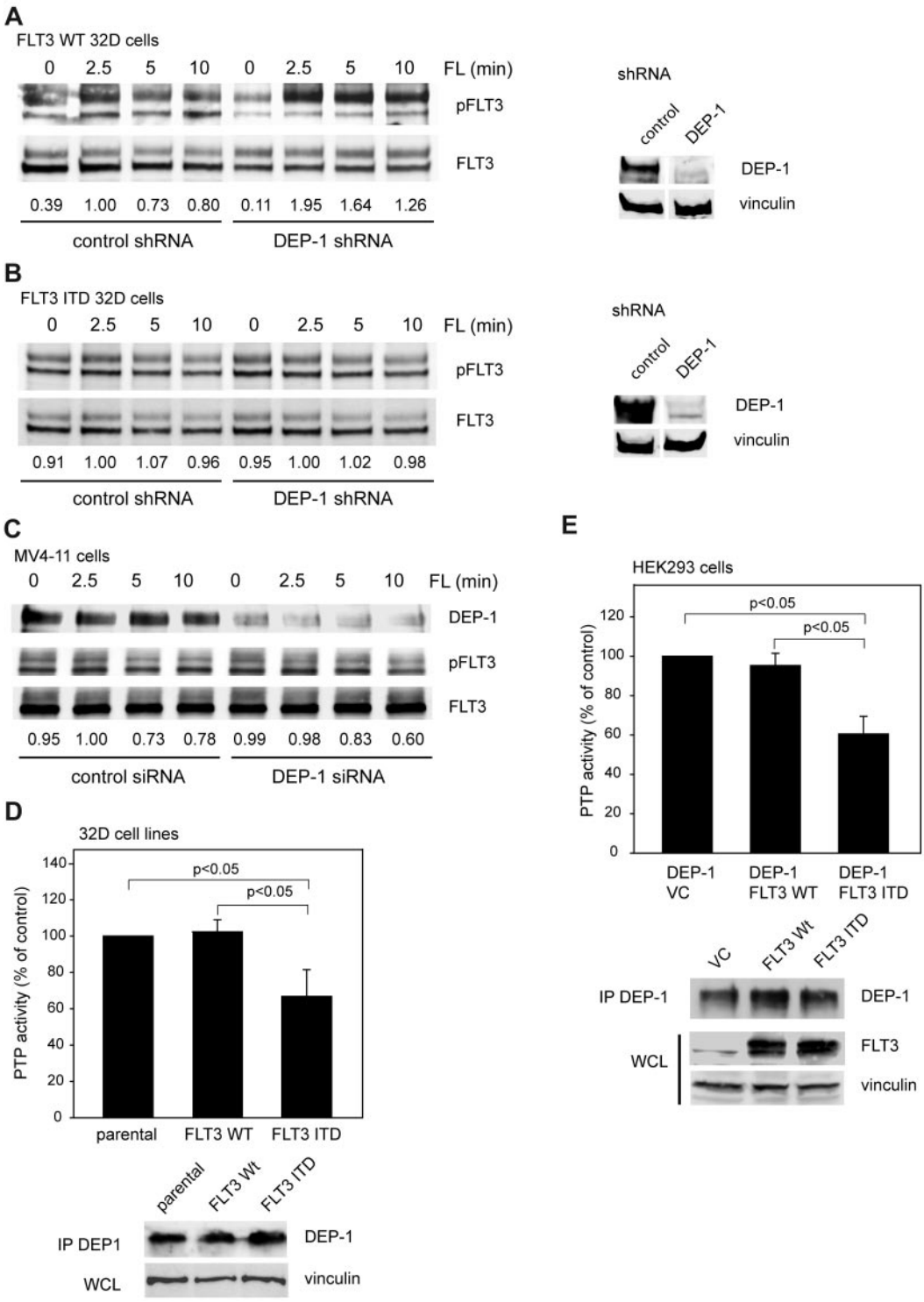

Figure 1. Dysfunction of DEP-1 in FLT3 ITD–expressing cells. 32D cells, either expressing WT FLT3 (A) or FLT3 ITD (B), which were stably transduced with nontargeting (control) or DEP-1 targeting shRNA (as indicated), or MV4-11 cells, transiently transfected with a DEP-1–targeting siRNA (C) were starved and stimulated with FLT3 ligand (FL) for the indicated time periods. FLT3 phosphorylation was assessed by immunoblotting in cell lysates with antibodies recognizing phosphorylated FLT3 (pFLT3, pY589, or pY591). Numbers under the blot indicate relative phosphorylation of FLT3, normalized to FLT3 amounts and to the value at 2.5 minutes stimulation in the control sh/siRNA-treated cells (1.0). Blots in the right panel reveal the DEP-1 knockdown in the used 32D cell pools, which were assayed in parallel to the signaling experiments. Note that blot sections are from the same membranes with identical exposure and image processing, but were rearranged for better clarity. DEP-1 activity was assayed in stably transfected 32D cells (D) or transiently transfected HEK293 cells (E) by measuring dephosphorylation of a phosphotyrosine-containing phosphopeptide with the malachite green assay in DEP-1 immunoprecipitates (values corrected for nonspecific precipitation with IgG controls; means of normalized values for 3 separate experiments ± standard deviation (SD), significance tested by *t* test). Cell lysis, immunoprecipitation, and activity assay were performed in an anaerobic chamber. Bottom panels verify equal DEP-1 protein levels.

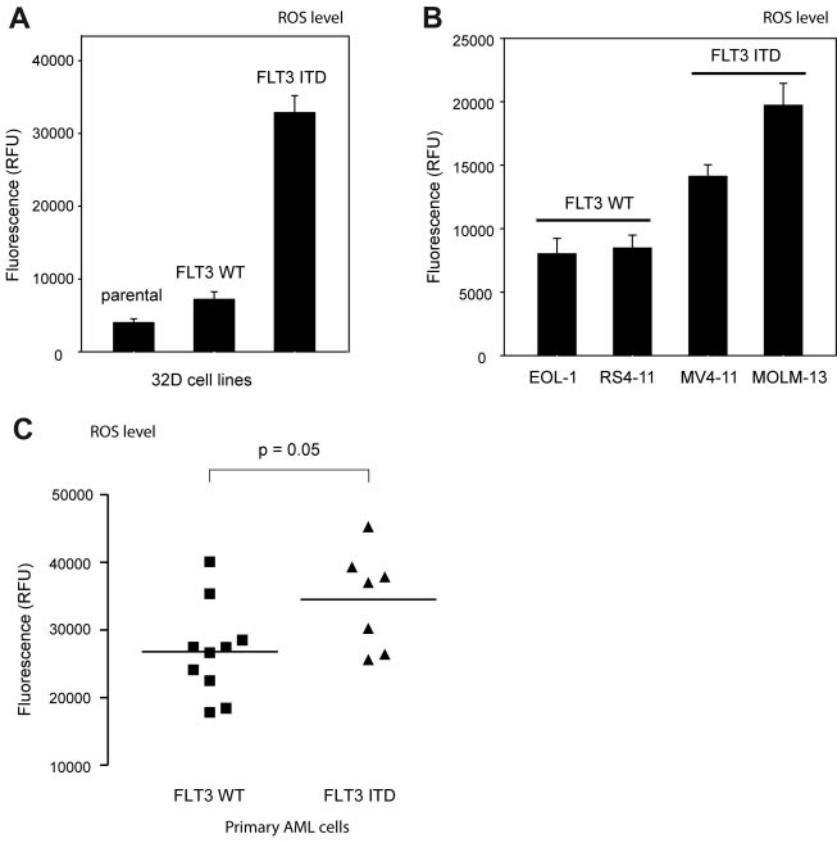

Figure 2. FLT3 ITD mediates generation of high levels of ROS. ROS production in 32D cells (A) or human myeloid cell lines (B) expressing either WT FLT3 or FLT3 ITD (as indicated) was measured with 2×10^6 cells per point using 5-(and-6)-carboxy-2′,7′-difluorodihydrofluorescein diacetate (carboxy-H_2DFFDA) in a fluorescence plate reader (mean $\pm$ SD, determination in triplicates, representative experiment of 3 with consistent results). (C) Elevated ROS production in AML patient blasts harboring FLT3 ITD. AML patient blasts were isolated from freshly taken blood samples. ROS levels were measured in a fluorescence plate reader using carboxy-H_2DFFDA. Values for 10 or 7 patients, harboring FLT3 WT or FLT3 ITD, respectively, are shown (significance tested by *t* test). Further data of the individual patients are provided in supplemental Figure 4.

inhibitory effect of FLT3 ITD expression on DEP-1 activity (Figure 3A), suggesting that H_2O_2 mediates the inactivation of DEP-1.

Further support for an involvement of oxidative inactivation of DEP-1 in FLT3 ITD cells was obtained in activity assays performed in the absence or presence of reducing agents. The activity of DEP-1 isolated from FLT3 ITD–overexpressing HEK293 cells could partially be recovered by treatment of the immunoprecipitates with dithiothreitol (DTT), indicating that the inactivation was at least partly because of reversible oxidation (Figure 3B).

To directly explore the effect of FLT3 ITD–mediated ROS production on the oxidation state of the DEP-1 catalytic cysteine, we used a previously reported alkylation approach.[23] In this assay increased PTP oxidation is detected as a reduced signal from the alkylating agent, which is only reacting with the reduced form of PTPs. As shown in Figure 3C, alkylation of DEP-1 with a biotin-labeled iodoacetic acid-derivative is greatly diminished in cells overexpressing FLT3 ITD, compared with WT FLT3–expressing cells. Coexpression of catalase led to enhanced alkylation, consistent with catalase-mediated rescue of PTP activity.

Furthermore, treatment of cells with DPI rescued activity of DEP-1 in the presence of FLT3 ITD, consistent with a potential role of NOX-derived ROS in the oxidation of DEP-1 in FLT3 ITD cells. Rescue of DEP-1 activity was detectable toward a synthetic phosphopeptide in DEP-1 immunoprecipitates (Figure 3D). Moreover, DEP-1 could dephosphorylate coexpressed FLT3 ITD in intact cells on activation by DPI treatment (Figure 3E). The latter experiment proved that the phosphotyrosines of FLT3 ITD are accessible to DEP-1, and that the initially observed defective regulation by DEP-1 was not caused by specific structural features of FLT3 ITD. It was also possible to force FLT3 ITD dephosphorylation in HEK293 cells by overexpression of DEP-1 to very high levels (data not shown). Consistent results were obtained with the more recently described NOX inhibitor VAS2870.[30] This compound inhibited ROS levels in FLT3 ITD–expressing 32D cells, and concomitantly led to substantial elevation of DEP-1 activity (Figure 3F).

It is probable that further PTPs contribute to regulation of FLT3 signaling activity. We therefore explored the effects of FLT3 ITD on activity of additional PTPs. We first tested PTP oxidation in 32D cells using a generic test, the modified in-gel PTP assay.[13] In this assay, reversibly oxidized PTPs can be detected based on their activity in sodium dodecyl sulfate (SDS)–polyacrylamide gel electrophoresis (PAGE) containing a [^{32}P]labeled substrate. Whereas cell treatment with H_2O_2 as a positive control caused abundant PTP oxidation, the presence of FLT3 ITD did not lead to any pronounced PTP oxidation detectable in this assay (Figure 4A). It should be noted that this assay is not suitable to detect activity of transmembrane PTPs such as DEP-1. We also used immunoprecipitation-based assays to assess the activity of PTP1B, a ubiquitously expressed nontransmembrane PTP, and of CD45, an abundant hematopoietic transmembrane PTP. Whereas the former was not affected in activity by coexpression of FLT3 ITD (Figure 4B), the latter showed only a trend of weakly reduced activity (Figure 4C). We also assessed another member of the PTP family, the lipid phosphatase and tensin homolog (PTEN). It negatively controls the PI3-kinase/AKT pathway, which is important for FLT3 ITD–mediated transformation.[31] Oxidation of PTEN has recently been shown in T-cell acute lymphoblastic leukemia cells.[29] PTEN oxidation can be detected based on a higher mobility of the oxidized species in nonreducing SDS-PAGE gels, and by a 2-step alkylation strategy leading to visualization of reversibly oxidized PTEN as a biotinylated species.[32] Both techniques did not reveal oxidized PTEN in FLT3 ITD–expressing cells (Figure 4D-F), whereas H_2O_2 readily caused PTEN oxidation. Although further PTPs need to be investigated, we concluded from these experiments that

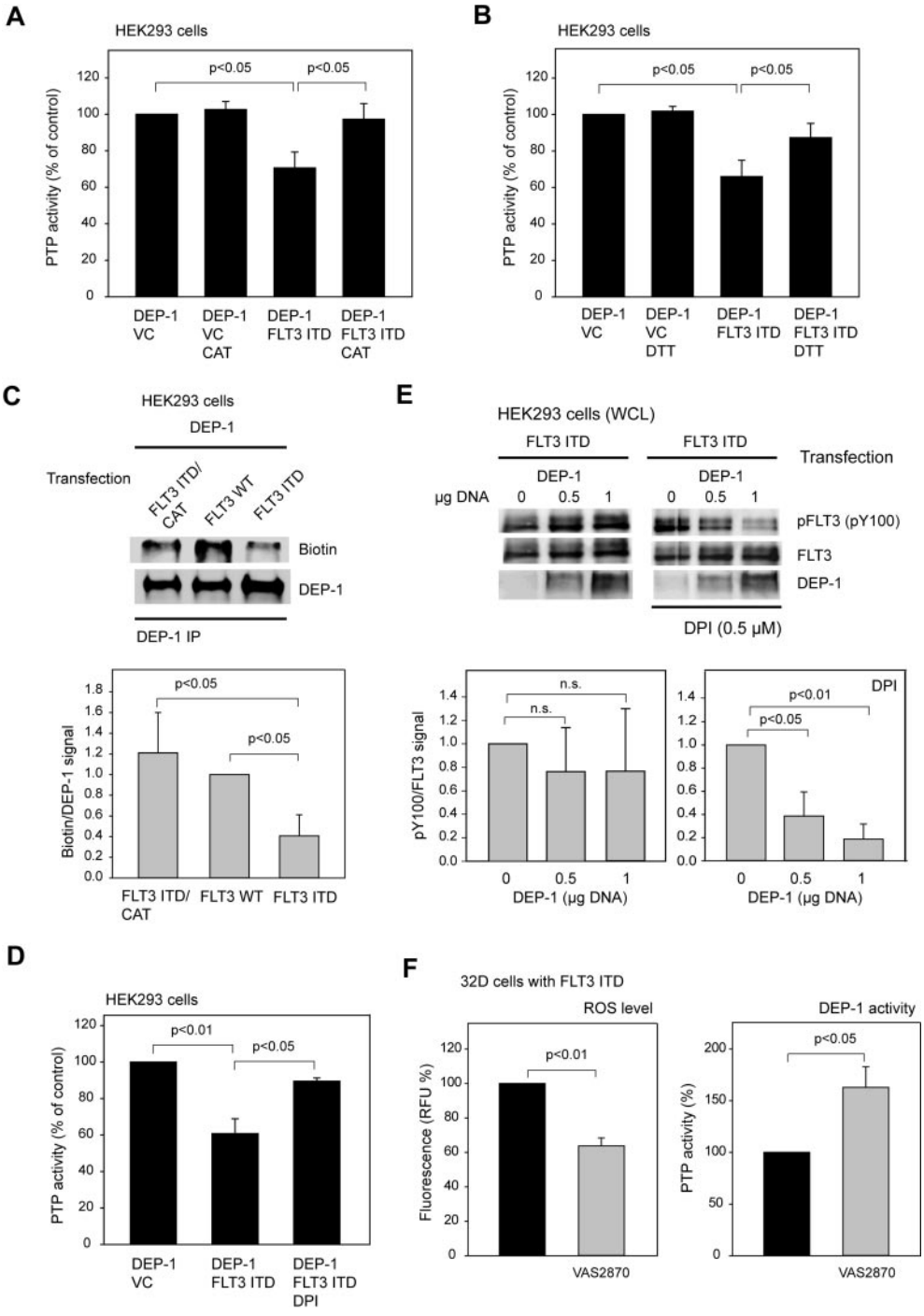

Figure 3. DEP-1 is inactivated by ROS in FLT3 ITD–expressing cells. (A) Rescue of DEP-1 activity by coexpression of catalase (CAT). The experiment was performed as in Figure 1E (means of normalized values for 3 separate experiments ± SD, significance tested by *t* test). (B) Partial recovery of DEP-1 activity by DTT treatment. DEP-1 was immunoprecipitated from HEK293 cells, which were transiently transfected as indicated. The immunoprecipitates were treated with 5mM DTT at room temperature for 10 minutes, or mock-incubated without DTT as indicated, then washed 3 times with PTP assay buffer, and the activity was subsequently assayed using the phosphopeptide substrate (values corrected for nonspecific precipitation with IgG controls; means of normalized values for 3 separate experiments ± SD, significance tested by *t* test). (C), FLT3 ITD causes ROS-mediated modification of the DEP-1 catalytic cysteine. HEK293 cells were transiently transfected with the indicated expression constructs, and lysed in the presence of biotinylated iodoacetate (EZ-link idoacetyl-PEG_2-biotin). DEP-1 was immunoprecipitated, and incorporation of biotin was assessed by immunoblotting. The blot was reprobed for comparable amounts of DEP-1. A representative experiment (top panel) and quantification of 3 experiments (means of normalized values for the ratio of signals for biotinylated DEP-1 and total DEP-1 ± SD, significance tested by *t* test, bottom panel) is shown. (D-E) DPI reactivates DEP-1 in FLT3 ITD–expressing cells. HEK293 cells were transiently transfected with the indicated expression constructs, and were left untreated or were treated with 0.5µM DPI for 6 hours before lysis. Thereafter, DEP-1 activity was assessed in immunoprecipitates (D; values corrected for nonspecific precipitation with IgG controls; means of normalized values for 3 separate experiments ± SD, significance tested by *t* test), or phosphorylation of FLT3 ITD was analyzed by immunoblotting (E). Top panel: representative experiment. Bottom panel: quantification of 3 separate exeriments (means of normalized values for the ratio of signals for phosphorylated FLT3 and total FLT3 ± SD, significance tested by *t* test). (F) VAS2870, a NADPH-oxidase inhibitor, reactivates DEP-1 in FLT3 ITD–expressing cells. FLT3 ITD–expressing 32D cells were treated with 50µM VAS2870 for 5 hours, thereafter ROS levels were determined using carboxy-H_2DFFDA and the DEP-1 activity was assayed measuring dephosphorylation of a phosphotyrosine-containing phosphopeptide with the malachite green assay in DEP-1 immunoprecipitates (means of normalized values for 3 separate experiments ± SD, significance tested by *t* test). Cell lysis, immunoprecipitation, and activity assay were performed in an anaerobic chamber.

DEP-1 oxidation appears as a relatively selective event. This notion is also supported by the finding that treatment of FLT3 ITD–expressing MOLM-13 cells with the general PTP inhibitor bV(phen) led to a remarkable elevation of both constitutive, and ligand-induced FLT3 autophosphorylation (Figure 4G). Although this is a very drastic treatment, which may cause nonspecific effects, the finding hints to other yet unidentifed PTPs controlling FLT3 phosphorylation, which are still functional in FLT3 ITD–expressing cells.

Inactivation of DEP-1 in FLT3 ITD–expressing primary AML cells

To address whether the model-derived findings presented were clinically relevant, we analyzed the possible relationship of ROS production and DEP-1 activity in leukemic cells isolated from the peripheral blood of AML patients harboring either WT FLT3 or FLT3 ITD.

Side-by-side comparison of multiple patient samples is hampered by the infrequent availability of fresh material, by the difficulty to cultivate these cells, and by unclear consequences of cell freezing for redox processes. Moreover, expression of DEP-1 is highly variable (supplemental Figure 2D). Presumably by the latter reason, comparison of basal DEP-1 activity in patient cells harboring WT FLT3 or FLT3 ITD revealed no statistically significant differences, however a clear trend to reduced activity in FLT3 ITD cells was observed (supplemental Figure 2E). To more rigorously test the impact of FLT3 ITD on DEP-1 activity, we therefore used a format, where untreated samples were side-by-side compared with samples treated with the FLT3 kinase inhibitor AG1295. This compound blocks ROS production downstream of FLT3 ITD as shown in supplemental Figure 3B-C. This assay was first validated in cell lines.

As shown in Figure 5A, treatment of the FLT3 ITD–harboring cell line MOLM-13 with AG1295 both led to reduction of ROS production, and to an elevation of DEP-1 activity. In contrast, AG1295-treatment of EOL-1 cells harboring WT FLT3 did not significantly change ROS production and DEP-1 activity was only weakly increased (Figure 5B). These data are consistent with the findings reported in the preceding paragraph, indicating that DEP-1 activity is inhibited by FLT3 ITD–driven ROS production.

The same assay was subsequently used on AML patient blasts. Interestingly, AG1295 caused reduced ROS levels and increased DEP-1 activity in FLT3 ITD–bearing blasts whereas no significant changes of this type were seen in patients with WT FLT3 (Figure 5C; see supplemental Figure 4 for individual patient data).

Taken together, these findings indicated that DEP-1 activity is indeed compromised by FLT3 ITD–driven ROS production in vitro and in vivo.

ROS-mediated DEP-1 inactivation contributes to transformation of 32D cells by FLT3 ITD

If the described DEP-1 inactivation were important for FLT3 ITD–driven transformation, interfering with ROS generation should inhibit transformation in the presence of DEP-1. This was tested using 32D cells stably expressing FLT3 ITD.

According to our preceding analysis, the NOX inhibitor DPI appeared to be a suitable agent because it effectively inhibited ROS production and restored DEP-1 activity. Because DPI also inhibits other flavoproteins and is toxic at high concentrations, we first carried out a titration experiment to estimate the minimal dose that would inhibit ROS substantially in these cells without severely impairing viability (supplemental Figure 5A). DPI (1 μM) inhibited ROS production by approximately 50% but attenuated the growth of FLT3 ITD–expressing cells only partially as revealed by proliferation assays (supplemental Figure 5B). The effect of this nontoxic dose of DPI was then assayed in colony formation assays. DPI strongly impaired colony formation under these conditions (Figure 6A).

If DEP-1 was involved in mediating this inhibition, one should expect refractoriness of DEP-1 deficient cells to this treatment. Indeed, stable DEP-1 depletion by shRNA partially prevented the inhibition of colony formation of FLT3 ITD expressing 32D cells (Figure 6A).

We also analyzed in parallel the effect of treatment with DPI on phosphorylation of STAT5, a prime mediator of transformation by FLT3 ITD. STAT5 phosphorylation was attenuated in the presence of DPI, providing biochemical evidence for the interference with a key transforming signaling step. However, the remaining STAT5 activity was obviously sufficient to sustain cell proliferation in suspension. The FLT3 ITD autophosphorylation was also reduced on DPI treatment in DEP-1 expressing cells, but to a much lesser extent in DEP-1–depleted cells (Figure 6B).

Similar results were obtained using the antioxidant TROLOX to interfere with the ROS pathway in FLT3 ITD cells. Again, TROLOX inhibited colony formation, and this effect was partially rescued by DEP-1 depletion (Figure 6C).

We finally attempted to stably interfere with ROS production, to assess effects on transformation in vivo. Stable overexpression was achieved for Prx-1, a potent H_2O_2-scavenging enzyme (supplemental Figure 5C). Prx-1–overexpressing 32D cells formed lesser colonies in presence of endogenous DEP-1, and this effect was partly abrogated in DEP-1–depleted cells (Figure 7A). We further confirmed that Prx-1 overexpression reduced ROS production in the stable cell pools, and caused elevation of DEP-1 activity (Figure 7B). When injected into syngeneic mice, the FLT3 ITD–expressing 32D cells caused rapid MPD, regardless of the depletion of DEP-1 (Figure 7C). However, on Prx-1 overexpression the development of MPD was significantly delayed for cells expressing DEP-1, whereas DEP-1–depleted cells were unaffected in their capacity to cause MPD (Figure 7C).

These data show that interference with the ROS production can attenuate transformation of 32D cells by FLT3 ITD in a DEP-1–dependent manner.

Discussion

Elimination of tumor suppressors by different molecular mechanisms, such as gene deletion, inactivating mutation, or silencing of transcription is a common phenomenon in oncogenesis. These mechanisms have been shown to operate also for tumor-suppressing PTPs, such as PTPRT, SHP-1, PTPRO,[33] PTPRD,[34,35] and recently TC-PTP.[36] We describe here another mechanism of eliminating a tumor suppressor PTP: the transforming kinase FLT3 ITD causes inactivation of the counteracting PTP DEP-1 via a ROS-mediated reversible oxidation of the catalytic cysteine. FLT3 ITD drives formation of high intracellular ROS levels via yet only partially understood pathways. As a consequence, DEP-1 becomes reversibly oxidized and thereby partially inactivated. This is detectable in experimental cell systems, but also in human AML cell lines harboring FLT3 ITD. On experimental restoration of DEP-1 activity by ROS scavenging, or Prx-1 overexpression, the transforming activity of FLT3 ITD is attenuated as revealed in 32D cells in vitro and in the related syngeneic mouse model of MPD.

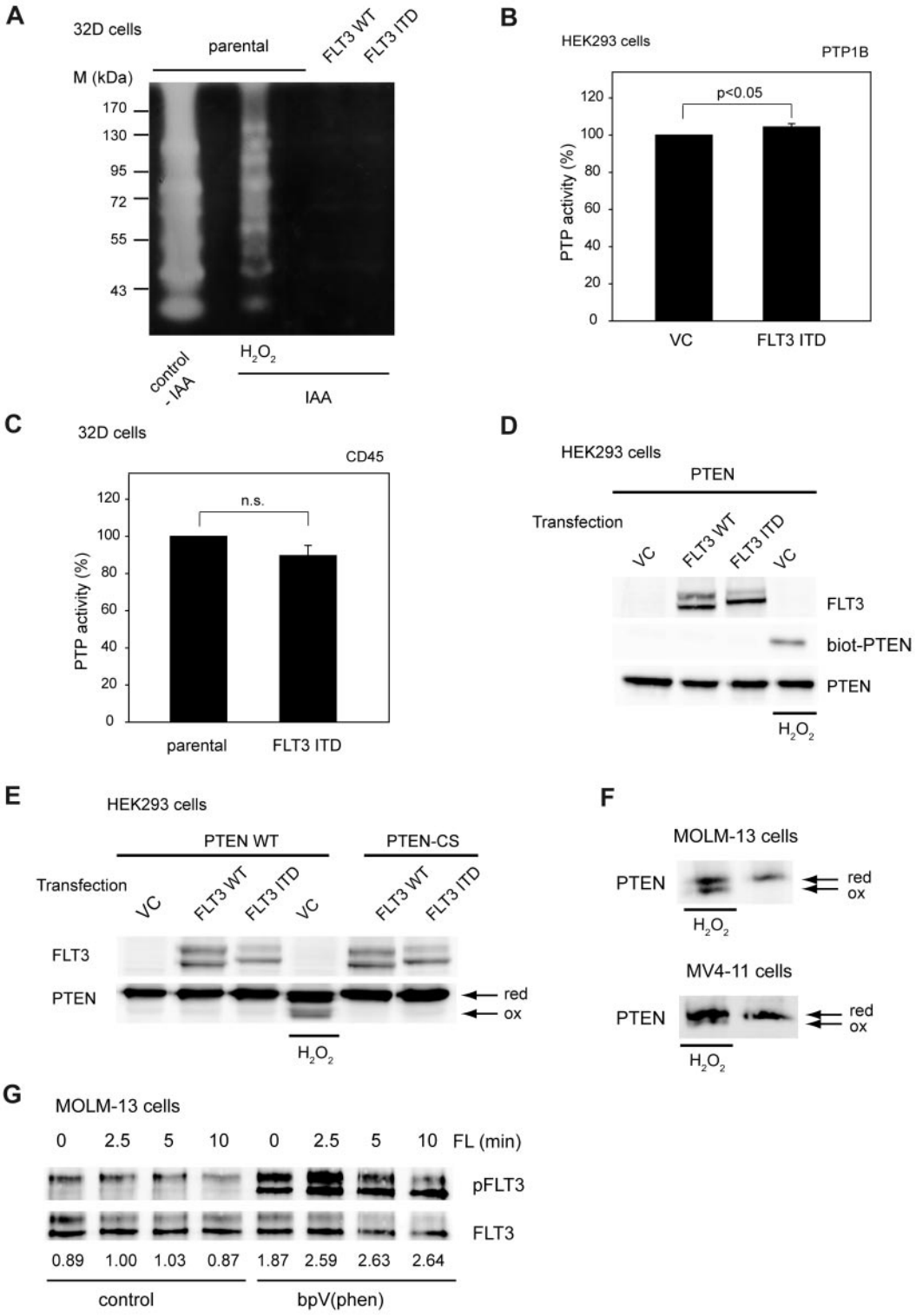

Figure 4. Activity of other protein-tyrosine phosphatases in FLT3 ITD–expressing cells. (A) Oxidation of cytoplasmic PTPs in 32D cells was assessed by the modified in-gel assay. Lysates of parental 32D cells, or 32D cells expressing WT FLT3 or FLT3 ITD (as indicated) were prepared in presence of the alkylant iodoacetic acid (IAA). For positive controls, parental 32D cells were pretreated with 1mM H_2O_2 for 10 minutes, and then lysed with IAA, or were lysed without IAA, as indicated. Lysate aliquots were separated in an SDS-PAGE gel containing [^{32}P]phosphotyrosine-poly(Glu_4Tyr), and the gels were processed for PTP renaturation, dried, and subjected to autoradiography. Subsequent to lysis in presence of IAA, only reversibly oxidized PTPs can be detected as white bands. Molecular masses are indicated. (B-C) The activity of the transmembrane PTP CD45 or PTP1B was also assessed in absence or presence of FLT3 ITD. (B) For PTP1B assays, endogenous PTP1B was immunoprecipitated from HEK293 cells, transiently transfected with control vector (VC) or an expression construct for FLT3 ITD. (C) For CD45 measurements, endogenous CD45 was immunoprecipitated from 32D cells stably expressing FLT3 ITD or parental 32D cells. Activity was measured in an anaerobic compartment by malachite green assays (values corrected for nonspecific precipitation with IgG controls; means of normalized values for 3 separate experiments ± SD, significance tested by *t* test). (D) Possible oxidation of the lipid phosphatase PTEN in presence of FLT3 ITD was assessed. HEK293 cells were transfected as indicated, and lysed in presence of the alkylating agents N-ethylmaleimide (NEM) and IAA in an anaerobic chamber. For positive control, one set of cells was also treated with 0.2mM H_2O_2 for 10 minutes before lysis. Proteins were precipitated with trichloroacetic acid to remove the alkylants, redissolved, subjected to reducing treatment, and subsequently reacted with biotin-conjugated maleimide. Biotinylated proteins were enriched with streptavidin-beads and analyzed by SDS-PAGE and immunoblotting. PTEN detected in this fraction was designated biot-PTEN.

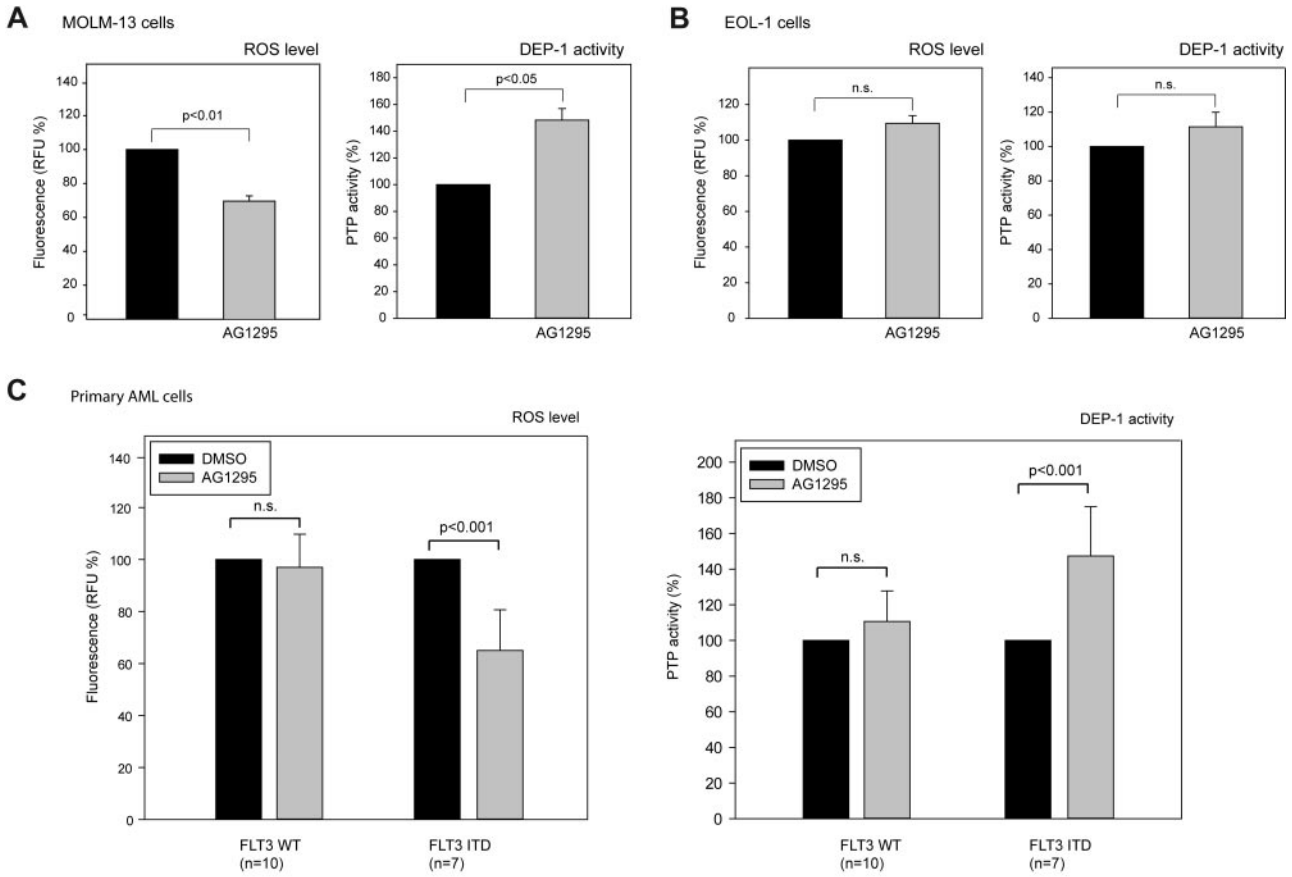

Figure 5. FLT3 ITD kinase-inhibition rescues DEP-1 activity in cell lines and AML patient blasts. The AML cell lines MOLM-13 (A), or EOL-1 (B), harboring FLT3 ITD, or WT FLT3, respectively, were treated with the FLT3 inhibitor AG1295 (20μM, 3 hours), or DMSO solvent, and subsequently ROS formation was measured in a plate reader using carboxy-H_2DFFDA (left panels). Endogenous DEP-1 was immunoprecipitated and assayed using a phosphopeptide substrate and malachite green detection (means of normalized values for 3 separate experiments ± SD, significance tested by *t* test). (C) AML patient blasts were freshly isolated from blood of patients taken before start of therapy. AG1295 treatment and measurement of ROS production and DEP-1 activity were performed as in (A-B). Values are based on duplicate (DEP-1 activity) and triplicate (ROS generation) determinations for each patient and means for all patients are presented (± SD, significance tested by *t* test). The data are normalized to values in vehicle (DMSO)–treated cells (100%). Data for ROS production and DEP-1 activity and the effects of AG1295 for individual patients are shown in supplemental Figure 4.

Our analysis of primary human cells revealed rather low expression of DEP-1 in normal hematopoietic progenitor ($CD34^+$) cells, and an apparent up-regulation to similar levels in both FLT3 ITD–positive and negative AML blasts by yet undefined mechanisms. In FLT3 ITD–expressing AML-cells, DEP-1 activity tended to be diminished by ROS-mediated inactivation compared with WT FLT3-expressing primary AML cells. Although these data are consistent with the findings in cell lines, further studies will be required to determine the contribution of DEP-1 oxidation to the pathogenesis of primary FLT3 ITD–positive AML.

PTP oxidation as a regulatory feed-forward mechanism to enable and enhance growth factor signaling was previously described.[17] Previous reports have also shown PTP oxidation in cancer cells, including even irreversible oxidation of PTP1B in A431 cells,[37] and of nontransmembrane and receptor-like PTPs in multiple cancer cell lines.[38,39] Based on the identification of DEP-1 as an efficient and relevant PTP for FLT3,[20] this study linked PTP oxidation to the activity of a critical oncoprotein in AML, FLT3 ITD.

One obvious question is the selectivity of PTP oxidation in FLT3 ITD–transformed cells. As shown in this study, 2 other PTPs are not inactivated in presence of FLT3 ITD: PTP1B, a nontransmembrane PTP residing largely in the endoplasmic reticulum, and CD45 an abundant transmembrane PTP in hematopoietic cells. Both PTPs have been shown previously to become oxidized in intact cells.[40-42] PTP1B is even among the PTPs which are most sensitive to oxidation by H_2O_2.[43] Likewise, we did not obtain evidence for oxidation of PTEN, a member of the PTP family with preferred activity for PIP3, in FLT3 ITD–expressing cells. Moreover, no abundant FLT3 ITD–mediated PTP oxidation was detectable using the generic method of the modified in-gel assay, which has been shown to reveal reversible oxidation of some cytoplasmic PTPs.[13] FLT3

Figure 4 (continued) Aliquots of fractions before the final affinity step were also analyzed as input controls (lowest panel). (E-F) HEK293 cells, which were transiently transfected as indicated (E), and MOLM-13 cells or MV4-11 cells expressing endogenously FLT3 ITD (F) were lysed in presence of 40mM NEM in an anaerobic chamber. Samples were fractionated by nonreducing SDS-PAGE. Oxidation of PTEN caused the formation of a band which migrates faster (designated ox) than the reduced form (red). For an additional specificity control, a PTEN cysteine-to-serine mutant (CS), which cannot become oxidized, was also analyzed. (G) MOLM-13 cells were serum-starved and treated with 100μM bV(phen), a general PTP inhibitor, for 15 minutes. Subsequently, cells were stimulated with FLT3 ligand (FL) for different time as indicated, lysed, and FLT3 was immunoprecipitated. Phosphorylation was analyzed by immunoblotting. Numbers under the blot indicate relative phosphorylation of the mature (top) FLT3 band, normalized to total FLT3 and phosphorylation at 2.5 minutes after FL-stimulation (1.0).

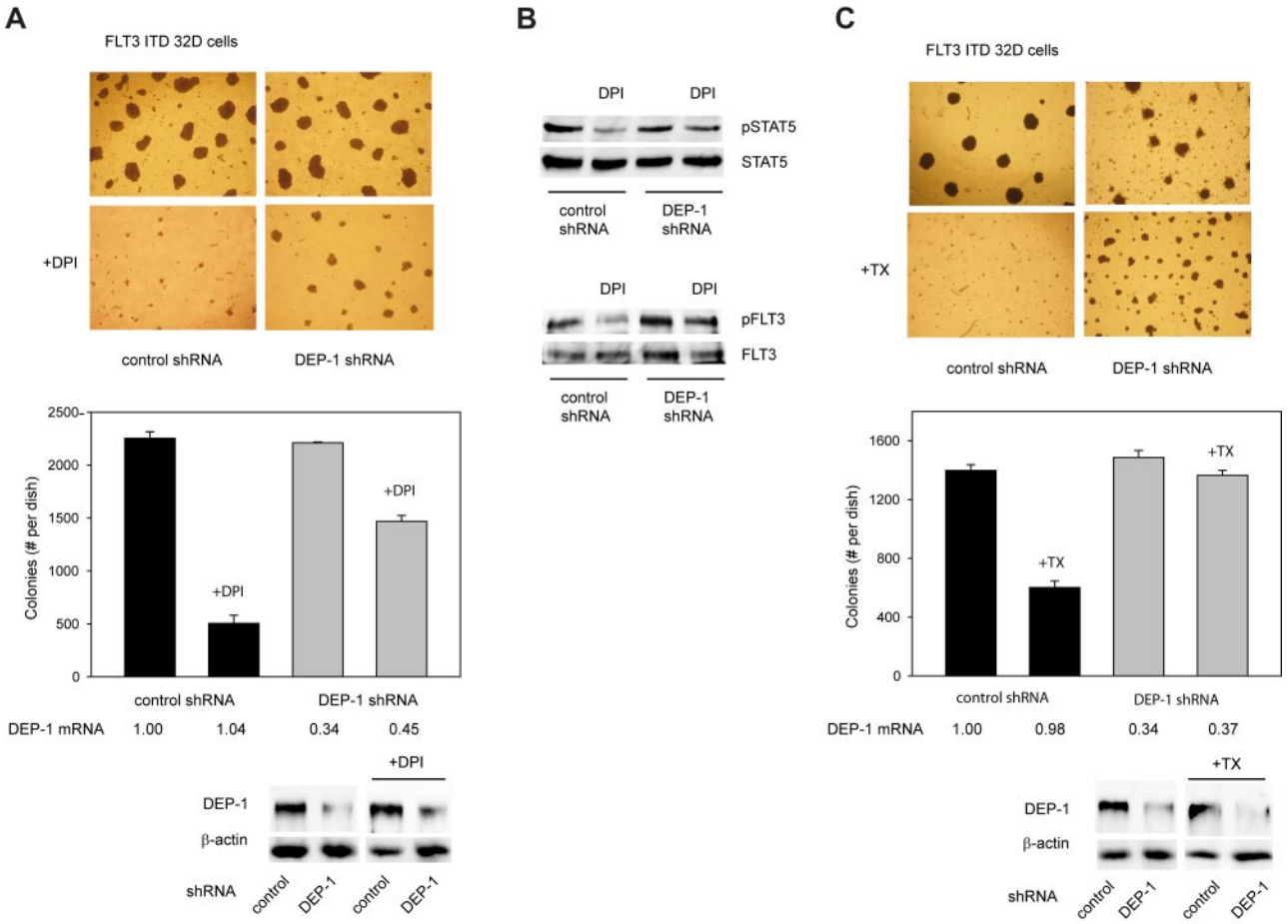

Figure 6. Pharmacologic inhibition of ROS formation inhibits FLT3 ITD–mediated cell transformation in a DEP-1–dependent manner. (A) 32D cells, stably transduced with FLT3 ITD, and additionally nontargeting shRNA (control), or DEP-1 targeting shRNA (as indicated), were subjected to colony formation assays in methylcellulose in absence or presence of 1μM DPI (as indicated) for 6 days. Left panel: example images. Pictures were taken with a 4× magnification objective lens using an Olympus CKX41 microscope equipped with a CAMEDIA C-7070 camera (Olympus). Right panel: quantification of colony formation. Only colonies > 0.4 mm were counted. Knockdown efficiencies were assessed by qRT-PCR and by immunoblotting after the treatment period, and are depicted under the graph. Note also equal DEP-1 expression levels in the cells harboring control shRNA. (B) The cells were treated with DPI or were mock-treated in suspension culture for 6 hours, and subsequently lysed and subjected to immunoblotting for assessing STAT5 (left panel) and FLT3 ITD (right panel) activation (representative experiment of 3 with consistent results). (C) Same experiment as in panel A, except that treatment was performed in absence or presence of 5mM TROLOX (TX).

hyperphosphorylation on cell treatment with a general PTP inhibitor argued even in favor of remaining FLT3-directed PTP activity in FLT3 ITD–expressing cells. We propose that selectivity for oxidation of DEP-1 versus CD45 and PTP1B and possibly further PTPs may be provided by a local production of ROS in the proximity of DEP-1. In intact cells, PTP oxidation is believed to require compartmentalization, and presumably also concurrent inactivation of ROS-decomposing systems, such as Prx enzymes.[44,45] However, we consider it probable that in addition to DEP-1 other yet unidentified PTPs are involved in dephosphorylation of FLT3. They may in part also be affected by oxidation in FLT3 ITD–expressing cells. There is substantial redundancy in PTP mediated regulation of RTKs.[10] Importantly, DEP-1 depletion in FLT3 ITD–expressing 32D cells made the cells only partially refractory to the effects of treatment with DPI or TROLOX, as well as Prx-1 overexpression. Interference with ROS production may also restore the activity of other affected PTPs. Continued search for FLT3-regulating PTPs will presumably identify further candidates for analysis of oxidation in FLT3 ITD cells.

It has been suggested by Sallmyr et al that downstream of FLT3 ITD activated STAT5 can recruit Rac1, in turn leading to increased ROS production.[8] Our data are also consistent with a role of STAT5, in addition to FLT3 ITD kinase activity, PI3K activity, and Rac1. A very recent study of the role of NOX enzymes in myeloid cells transformed by oncogenic tyrosine kinases reported elevated metabolic activity, increased mitochondrial ROS production, and elevated NADPH levels downstream of FLT3 ITD kinase activity.[9] Further elucidation of the yet incompletely understood pathways leading to ROS production will be required, and may also provide insights into the localization of the ROS source(s) relative to DEP-1. The identity of the ROS, which directly oxidizes DEP-1, is likewise not yet clear. ROS detection with pHyPer, and in particular, our experiments with catalase indicate an important role of H_2O_2, consistent with previous findings.[46] However, this does not exclude the importance of additional intermediates, such as lipid oxidation products.[47]

It has been recently shown that elevated ROS in FLT3 ITD–transformed cells promotes formation of DNA double-strand breaks[8] and the frequency of mutagenic single-strand annealing DNA repair.[48] These effects of ROS are considered to lead to accumulation of mutations, which may collaborate with FLT3 ITD in transformation. The nonnuclear action of ROS described here will instead contribute acutely to transformation by FLT3 ITD. Both processes are clearly not mutually exclusive.

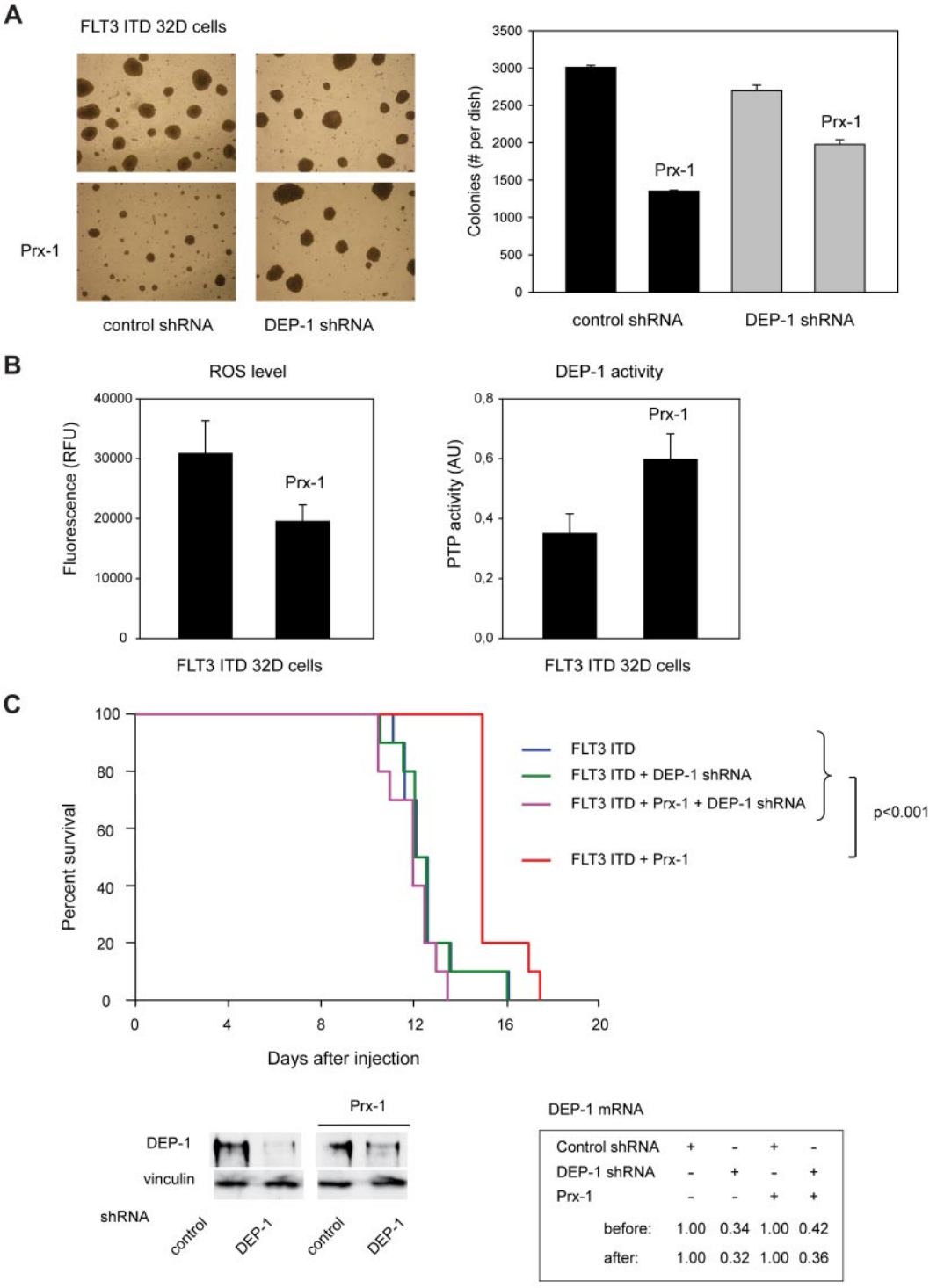

Figure 7. Reactivation of DEP-1 by Prx-1 overexpression attenuates FLT3 ITD–dependent transformation. FLT3 ITD expressing 32D cells, harboring either nontargeting shRNA (not labeled for better clarity in panel C) or DEP-1 targeting shRNA (as indicated), were engineered by retroviral transduction to overexpress Prx-1, or were transduced with control vector. (A) Colony formation in methylcellulose of the 4 different cell pools was assessed. Left panel: example image. Right panel: quantification of colonies > 0.4 mm. (B) ROS formation and DEP-1 activity were assessed as described for Figures 2A and 1C, respectively (representative experiments of 3 with consistent results). (C) C3H/HeJ mice (10 mice per group) were injected with 2×10^6 cells each of the indicated 32D cell pools. Survival was monitored and is displayed as Kaplan-Meier plot. Statistical significance was tested using Gehan-Breslow statistics for the survival curves; posthoc comparisons were made with the Holm-Sidak method for all pairwise multiple comparisons. DEP-1 knockdown efficiencies were assessed at day 11 as described in "Methods," and are shown as qRT-PCR and immunoblotting data in the bottom panels. Note also equal DEP-1 expression in the cell pools harboring control shRNA. Survival of mice injected with cells harboring FLT3 ITD and Prx-1 was significantly prolonged (15.4 $\pm$ 0.3 days; $P < .001$) compared with mice injected with the corresponding cells additionally harboring DEP-1 shRNA (11.9 $\pm$ 0.3 days), with cells harboring FLT3 ITD but without Prx-1 12.5 $\pm$ 0.4 days), and with cells harboring FLT3 ITD and DEP-1 shRNA only (12.5 $\pm$ 0.2 days). There was no significant difference in the survival curves of mice injected with the latter 3 cell types.

ROS quenching has been considered as a therapeutic strategy in cancer.[49] Further work will be required to establish the relevance of ROS-mediated inactivation of DEP-1 and possibly other PTPs for human AML, and whether ROS quenching may be a viable therapeutic strategy in this disease.

Acknowledgments

The authors are grateful to Drs Nolan, Duyster, Lambeth, Pfitzner, Rönnstrand, and Ungefroren, and the Vasopharm company for the kind provision of cells or reagents; and to Peter Herrlich for critical reading of the paper and stimulating discussions throughout this project.

This work was supported by the Deutsche Forschungsgemeinschaft (BO1043/6-3), the Deutsche Krebshilfe (Collaborative grant 108401, TP2 to F.D.B.), and the European Community ("PTP-NET" Marie Curie Network MRTN-CT-2006-035830, to F.D.B. and A.Ö.).

Authorship

Contribution: R.G. designed and performed experiments, analyzed the data, and wrote parts of the paper; D.A., R.B., S.S., T.H., S.A.B., J.P.M., M.D., and U.S. did experiments; S.S. characterized and provided clinical samples; A.Ö. contributed to concept and the paper; and F.-D.B. planned and supervised the study, and wrote the paper.

Conflict of interest disclosure: The authors declare no competing financial interests.

The current affiliation for R.G. is Molecular Cardiology and Angiology, University Hospital Münster, Münster, Germany.

Correspondence: F.-D. Böhmer, Institute of Molecular Cell Biology, Hans-Knöll-Strasse 2, D-07745 Jena, Germany; e-mail: boehmer@med.uni-jena.de.

References

1. Fröhling S, Scholl C, Gilliland DG, Levine RL. Genetics of myeloid malignancies: pathogenetic and clinical implications. *J Clin Oncol.* 2005;23(26):6285-6295.
2. Döhner H, Estey EH, Amadori S, et al. Diagnosis and management of acute myeloid leukemia in adults: recommendations from an international expert panel, on behalf of the European LeukemiaNet. *Blood.* 2010;115(3):453-474.
3. Meshinchi S, Appelbaum FR. Structural and functional alterations of FLT3 in acute myeloid leukemia. *Clin Cancer Res.* 2009;15(13):4263-4269.
4. Breitenbuecher F, Schnittger S, Grundler R, et al. Identification of a novel type of ITD mutations located in nonjuxtamembrane domains of the FLT3 tyrosine kinase receptor. *Blood.* 2009;113(17):4074-4077.
5. Kayser S, Schlenk RF, Londono MC, et al. Insertion of FLT3 internal tandem duplication in the tyrosine kinase domain-1 is associated with resistance to chemotherapy and inferior outcome. *Blood.* 2009;114(12):2386-2392.
6. Grundler R, Miething C, Thiede C, Peschel C, Duyster J. FLT3-ITD and tyrosine kinase domain mutants induce 2 distinct phenotypes in a murine bone marrow transplantation model. *Blood.* 2005;105(12):4792-4799.
7. Schmidt-Arras D, Bohmer SA, Koch S, et al. Anchoring of FLT3 in the endoplasmic reticulum alters signaling quality. *Blood.* 2009;113(15):3568-3576.
8. Sallmyr A, Fan J, Datta K, et al. Internal tandem duplication of FLT3 (FLT3/ITD) induces increased ROS production, DNA damage, and misrepair: implications for poor prognosis in AML. *Blood.* 2008;111(6):3173-3182.
9. Reddy MM, Fernandes MS, Salgia R, Levine RL, Griffin JD, Sattler M. NADPH oxidases regulate cell growth and migration in myeloid cells transformed by oncogenic tyrosine kinases. *Leukemia.* 2011;25(2):281-289.
10. Östman A, Bohmer FD. Regulation of receptor tyrosine kinase signaling by protein tyrosine phosphatases. *Trends Cell Biol.* 2001;11(6):258-266.
11. den Hertog J, Ostman A, Bohmer FD. Protein tyrosine phosphatases: regulatory mechanisms. *FEBS J.* 2008;275(5):831-847.
12. Denu JM, Tanner KG. Specific and reversible inactivation of protein tyrosine phosphatases by hydrogen peroxide: evidence for a sulfenic acid intermediate and implications for redox regulation. *Biochemistry.* 1998;37(16):5633-5642.
13. Meng TC, Fukada T, Tonks NK. Reversible oxidation and inactivation of protein tyrosine phosphatases in vivo. *Mol Cell.* 2002;9(2):387-399.
14. Tonks NK. Redox redux: revisiting PTPs and the control of cell signaling. *Cell.* 2005;121(5):667-670.
15. Lambeth JD. NOX enzymes and the biology of reactive oxygen. *Nat Rev Immunol.* 2004;4(3):181-189.
16. Stone JR, Yang S. Hydrogen peroxide: a signaling messenger. *Antioxid Redox Signal.* 2006;8(3-4):243-270.
17. Rhee SG, Kang SW, Jeong W, Chang TS, Yang KS, Woo HA. Intracellular messenger function of hydrogen peroxide and its regulation by peroxiredoxins. *Curr Opin Cell Biol.* 2005;17(2):183-189.
18. Schmidt-Arras DE, Bohmer A, Markova B, Choudhary C, Serve H, Böhmer FD. Tyrosine phosphorylation regulates maturation of receptor tyrosine kinases. *Mol Cell Biol.* 2005;25(9):3690-3703.
19. Möller JP, Schonherr C, Markova B, Bauer R, Stocking C, Böhmer FD. Role of SHP2 for FLT3-dependent proliferation and transformation in 32D cells. *Leukemia.* 2008;22(10):1945-1948.
20. Arora D, Stopp S, Bohmer SA, et al. Protein tyrosine phosphatase DEP-1 controls receptor tyrosine kinase FLT3 signaling. *J Biol Chem.* 2011;286(13):10918-10929.
21. Karagyozov L, Godfrey R, Bohmer SA, et al. The structure of the 5′-end of the protein-tyrosine phosphatase PTPRJ mRNA reveals a novel mechanism for translation attenuation. *Nucleic Acids Res.* 2008;36(13):4443-4453.
22. Sandin A, Dagnell M, Gonon A, et al. Hypoxia followed by re-oxygenation induces oxidation of tyrosine phosphatases. *Cell Signal.* 2011;23(5):820-826.
23. Chen K, Kirber MT, Xiao H, Yang Y, Keaney JF Jr. Regulation of ROS signal transduction by NADPH oxidase 4 localization. *J Cell Biol.* 2008;181(7):1129-1139.
24. Lin J, Zhu JW, Baker JE, Weiss A. Regulated expression of the receptor-like tyrosine phosphatase CD148 on hemopoietic cells. *J Immunol.* 2004;173(4):2324-2330.
25. Arimura Y, Yagi J. Comprehensive expression profiles of genes for protein tyrosine phosphatases in immune cells. *Sci Signal.* 2010;3(137):rs1.
26. de Jonge HJ, Woolthuis CM, Vos AZ, et al. Gene expression profiling in the leukemic stem cell-enriched CD34(+) fraction identifies target genes that predict prognosis in normal karyotype AML. *Leukemia.* 2011;25(12):1825-1833.
27. Markvicheva KN, Bogdanova EA, Staroverov DB, Lukyanov S, Belousov VV. Imaging of intracellular hydrogen peroxide production with HyPer upon stimulation of HeLa cells with epidermal growth factor. *Methods Mol Biol.* 2008;476:79-86.
28. Lambeth JD, Krause KH, Clark RA. NOX enzymes as novel targets for drug development. *Semin Immunopathol.* 2008;30(3):339-363.
29. Müller J, Sperl B, Reindl W, Kiessling A, Berg T. Discovery of chromone-based inhibitors of the transcription factor STAT5. *Chembiochem.* 2008;9(5):723-727.
30. Freyhaus H, Huntgeburth M, Wingler K, et al. Novel Nox inhibitor VAS2870 attenuates PDGF-dependent smooth muscle cell chemotaxis, but not proliferation. *Cardiovasc Res.* 2006;71(2):331-341.
31. Brandts CH, Sargin B, Rode M, et al. Constitutive activation of Akt by Flt3 internal tandem duplications is necessary for increased survival, proliferation, and myeloid transformation. *Cancer Res.* 2005;65(21):9643-9650.
32. Kwon J, Lee SR, Yang KS, et al. Reversible oxidation and inactivation of the tumor suppressor PTEN in cells stimulated with peptide growth factors. *Proc Natl Acad Sci U S A.* 2004;101(47):16419-16424.
33. Ostman A, Hellberg C, Bohmer FD. Protein-tyrosine phosphatases and cancer. *Nat Rev Cancer.* 2006;6(4):307-320.
34. Solomon DA, Kim JS, Cronin JC, et al. Mutational inactivation of PTPRD in glioblastoma multiforme and malignant melanoma. *Cancer Res.* 2008;68(24):10300-10306.
35. Veeriah S, Brennan C, Meng S, et al. The tyrosine phosphatase PTPRD is a tumor suppressor that is frequently inactivated and mutated in glioblastoma and other human cancers. *Proc Natl Acad Sci U S A.* 2009;106(23):9435-9440.
36. Kleppe M, Lahortiga I, El Chaar T, et al. Deletion of the protein tyrosine phosphatase gene PTPN2 in T-cell acute lymphoblastic leukemia. *Nat Genet.* 2010;42(6):530-535.
37. Lou YW, Chen YY, Hsu SF, et al. Redox regulation of the protein tyrosine phosphatase PTP1B in cancer cells. *FEBS J.* 2008;275(1):69-88.
38. Boivin B, Zhang S, Arbiser JL, Zhang ZY, Tonks NK. A modified cysteinyl-labeling assay reveals reversible oxidation of protein tyrosine phosphatases in angiomyolipoma cells. *Proc Natl Acad Sci U S A.* 2008;105(29):9959-9964.
39. Karisch R, Fernandez M, Taylor P, et al. Global proteomic assessment of the classical protein-tyrosine phosphatome and "Redoxome". *Cell.* 2011;146(5):826-840.

40. Lee SR, Kwon KS, Kim SR, Rhee SG. Reversible inactivation of protein-tyrosine phosphatase 1B in A431 cells stimulated with epidermal growth factor. *J Biol Chem.* 1998;273(25):15366-15372.

41. Galic S, Hauser C, Kahn BB, et al. Coordinated regulation of insulin signaling by the protein tyrosine phosphatases PTP1B and TCPTP. *Mol Cell Biol.* 2005;25(2):819-829.

42. Rider DA, Sinclair AJ, Young SP. Oxidative inactivation of CD45 protein tyrosine phosphatase may contribute to T lymphocyte dysfunction in the elderly. *Mech Ageing Dev.* 2003;124(2):191-198.

43. Groen A, Lemeer S, van der Wijk T, et al. Differential oxidation of protein-tyrosine phosphatases. *J Biol Chem.* 2005;280(11):10298-10304.

44. Winterbourn CC. Reconciling the chemistry and biology of reactive oxygen species. *Nat Chem Biol.* 2008;4(5):278-286.

45. Woo HA, Yim SH, Shin DH, Kang D, Yu DY, Rhee SG. Inactivation of peroxiredoxin I by phosphorylation allows localized H(2)O(2) accumulation for cell signaling. *Cell.* 2010;140(4):517-528.

46. Juarez JC, Manuia M, Burnett ME, et al. Superoxide dismutase 1 (SOD1) is essential for H2O2-mediated oxidation and inactivation of phosphatases in growth factor signaling. *Proc Natl Acad Sci U S A.* 2008;105(20):7147-7152.

47. Conrad M, Sandin A, Forster H, et al. 12/15-lipoxygenase-derived lipid peroxides control receptor tyrosine kinase signaling through oxidation of protein tyrosine phosphatases. *Proc Natl Acad Sci U S A.* 2010;107(36):15774-15779.

48. Fernandes MS, Reddy MM, Gonneville JR, et al. BCR-ABL promotes the frequency of mutagenic single-strand annealing DNA repair. *Blood.* 2009;114(9):1813-1819.

49. Wondrak GT. Redox-directed cancer therapeutics: molecular mechanisms and opportunities. *Antioxid Redox Signal.* 2009;11(12):3013-3069.